

Iodo bridged lead(II) compounds of azoimidazoles:
Single crystal X-ray structures of
[di-iodo- $\{1\text{-methyl-2-}(p\text{-tolylazo})\text{imidazole}\}\text{lead(II)}\}_n$ and
 $\{1\text{-methyl-3-benzyl-2-}(p\text{-tolylazo})\text{imidazolium}\}_m$ -
 $\{\text{tri-iodoplumbate(II)}\}_m$

K.K. Sarker ^a, A.D. Jana ^b, G. Mostafa ^b, J.-S. Wu ^c, T.-H. Lu ^c, C. Sinha ^{a,*}

^a Department of Chemistry, Inorganic Chemistry Section, Jadavpur University, Raja Suboth Mullick Road, Kolkata 700 032, West Bengal, India

^b Department of Physics, Jadavpur University, Kolkata 700 032, West Bengal, India

^c Department of Physics, National Tsing Hua University, Hsinchu 300, Taiwan, ROC

Received 17 March 2006; received in revised form 19 May 2006; accepted 28 May 2006

Available online 9 June 2006

Abstract

PbI₂ forms iodo-bridged neutral polymer upon reaction with 1-alkyl-2-(arylo)imidazoles (RaaiR'). The reaction of PbI₂ and dialkyl imidazolium iodides [RaaiR'R'']⁺I⁻ has synthesized $\{1,3\text{-dialkyl-2-}(arylo)\text{imidazolium}\}_m\text{-}\{\text{tri-iodoplumbate(II)}\}_m$. The complexes are characterized by different spectroscopic studies. Iodobridged chelated polymer, [Pb(RaaiR')I₂]_n, has been established by single crystal X-ray diffraction measurements in one case. Tri-iodoplumbates form iodo bridged anion polymer, which connects [RaaiR'R'']⁺ by hydrogen bonding and are placed in between the pillars of [Pb(μ-I)₆]_n motif.

© 2006 Elsevier B.V. All rights reserved.

Keywords: Pb(II)-iodo complexes; Aryloimidazole; Azoimidazolium; X-ray structures

1. Introduction

In the recent years, inorganic–organic hybrid compounds have attracted attention as an effective way to generate useful material of high mechanical and dimensional stability. Metal ions display a range of coordination geometries allowing for greater flexibility in constructing materials with specific dimensions and topologies [1–9]. Halo compounds of metals with d¹⁰ configuration show various coordination numbers and configuration [10]. It is observed that chloro compounds are commonly bridged polymeric but the bromo and iodo derivatives are usually monomeric. Iodo compounds often behave differently in

terms of the structure, chemical, photophysical and redox properties. It has been suggested that the tendency of iodine to reduce coordination number of the metal atom is due to an increase in electron density at the metal center caused by softer character and larger size of iodine relative to lighter halogen [11,12]. Although I⁻ is reluctant, in general, to generate polymeric network with most of the metal ions but Cu(I), Ag(I) form myriad of iodine bridged dimers, cubanes, chains, strands, etc. [10,13]. Major disadvantage of the M–I bonding is the very high electronic flexibility that is being influenced significantly by the coligands compared to the M–Cl/Br bonds [14,15]. This has reasoned to undertake the iodo complexes of lead (reasonable heavy toxic metal) with chelating ligands. PbI₂ and iodoplumbates are efficient photosensitizers and the thin films of these compounds are studied for long time [16]. The lead (II) complexes are interesting and are frequently discussed

* Corresponding author. Tel.: +91 94 3330 9907; fax: +91 33 2414 6584, 91 33 2413 7121.

E-mail address: c_r_sinha@yahoo.com (C. Sinha).

to consider the coordination and stereoactivity of heavy metals, in particular, to the ‘stereochemical activity’ of valence shell electron lone pairs [17–19]. The lead(II) complexes of polypyridine systems have been studied only recently [20,21].

Our present programme is to explore the transition and non-transition metal-iodo complexes of 1-alkyl-2-(arylazo)imidazoles. Studies on the pseudohalide complexes of transition [22–25] and non-transition [26–29] metals with 1-alkyl-2-(arylazo)imidazole have been discussed recently by us. The end capping role of the chelating ligand in combination with the $\pi \cdots \pi$ and C–H $\cdots \pi$ interaction has led to synthesize coordination polymers of different dimensionality [30–33]. Arylazoimidazolium ions have selectively bonded with anions like ReO_4^- [34,35]. This has encouraged us to synthesize iodoplumbates of arylazoimidazolium system. The compounds are characterized by spectroscopic techniques and the structural confirmation has been carried out by single crystal X-ray diffraction studies.

2. Experimental

2.1. Materials

Imidazole, different aromatic amines, and $\text{Pb}(\text{NO}_3)_2$ were purchased from E. Merck India. PbI_2 was prepared freshly from the mixture of $\text{Pb}(\text{NO}_3)_2$ and KI, and washed with water just before use. All other chemicals and solvents were of reagent grade and used as received. 1-Alkyl-2-(arylazo)imidazole (RaaiR') were prepared by the reported procedure [22–25].

2.2. Physical measurements

Microanalytical (C, H, N) data were obtained from a Perkin–Elmer 2400 CHNS/O elemental analyzer. Spectroscopic data were obtained using the following instruments: UV–Vis, Perkin–Elmer Lambda-25; IR (KBr disk, 4000–200 cm^{-1}), Perkin–Elmer RX-1 spectrophotometer, and ^1H NMR, Bruker 300 MHz FT-NMR spectrometer.

2.3. Preparation of compounds

2.3.1. Synthesis of $[\text{Pb}(\text{MeaiMe})(\text{I})_2]_n$ (**8b**)

1-Methyl-2-(*p*-tolylazo)imidazole (0.05 g, 0.25 mmol) in MeOH (15 ml) was added dropwise to a stirred ethylene glycol monomethyl ether solution (15 ml) of PbI_2 (0.057 g, 0.12 mmol) at room temperature. The color was changed to red-orange. The solution was then refluxed for 2 h and red-orange crystalline compound was found deposited on the glass surface. The solution was filtered hot and allowed to evaporate slowly. Bright red-orange crystals were obtained after a week. The crystals were collected by filtration and washed with methanol. The crystals were dissolved in a minimum volume of 2-methoxy-ethanol and two volumes of methanol was added into it. The resulting mixture was then allowed to evaporate slowly. The

crystals were collected and were suitable for single crystal X-ray study. The yield was 0.11 g (67%).

All other complexes were prepared by the same procedure. In all cases, crystalline products were obtained. The yield varied from 60% to 75%. The microanalytical data of the complexes are as follows, $[\text{Pb}(\text{HaaiMe})(\text{I})_2]_n$ (**8a**): *Anal. Calc.* for $\text{C}_{10}\text{H}_{10}\text{N}_4\text{I}_2\text{Pb}$: C, 18.54; H, 1.55; N, 8.65. Found: C, 18.60; H, 1.50; N, 8.70%. FT-IR (KBr disc, cm^{-1}), $\nu(\text{N}=\text{N})$, 1430; $\nu(\text{C}=\text{N})$, 1588 cm^{-1} . UV–Vis spectral data in DMF [$\lambda_{\text{max}}(\text{nm})(10^{-3}\epsilon(\text{dm}^3 \text{mol}^{-1} \text{cm}^{-1}))$]: 260 (14.10), 370 (13.10), 390 (12.90), 460 (0.45). $[\text{Pb}(\text{MeaiMe})(\text{I})_2]_n$ (**8b**): *Anal. Calc.* for $\text{C}_{11}\text{H}_{12}\text{I}_2\text{N}_4\text{Pb}$: C, 19.96; H, 1.81; N, 8.47. Found: C, 19.90; H, 1.86; N, 8.40%. FT-IR (KBr disc, cm^{-1}), $\nu(\text{N}=\text{N})$, 1436; $\nu(\text{C}=\text{N})$, 1597 cm^{-1} . UV–Vis spectral data in DMF [$\lambda_{\text{max}}(\text{nm})(10^{-3}\epsilon(\text{dm}^3 \text{mol}^{-1} \text{cm}^{-1}))$]: 262 (1.50), 368 (4.12), 384 (3.84), 412 (1.42), 464 (0.54). $[\text{Pb}(\text{HaaiEt})(\text{I})_2]_n$ (**9a**): *Anal. Calc.* for $\text{C}_{11}\text{H}_{12}\text{I}_2\text{N}_4\text{Pb}$: C, 19.96; H, 1.81; N, 8.47. Found: C, 20.02; H, 1.76, N, 8.40%. FT-IR (KBr disc, cm^{-1}), $\nu(\text{N}=\text{N})$, 1437; $\nu(\text{C}=\text{N})$, 1588 cm^{-1} . UV–Vis spectral data in DMF [$\lambda_{\text{max}}(\text{nm})(10^{-3}\epsilon(\text{dm}^3 \text{mol}^{-1} \text{cm}^{-1}))$]: 268 (7.40), 294 (3.60), 364 (13.00), 390 (8.98), 467 (0.25). $[\text{Pb}(\text{MeaiEt})(\text{I})_2]_n$ (**9b**): *Anal. Calc.* for $\text{C}_{12}\text{H}_{14}\text{I}_2\text{N}_4\text{Pb}$: C, 21.33; H, 2.07; N, 8.29. Found: C, 21.40; H, 2.02; N, 8.20%. FT-IR (KBr disc, cm^{-1}), $\nu(\text{N}=\text{N})$, 1439; $\nu(\text{C}=\text{N})$, 1597 cm^{-1} . UV–Vis spectral data in DMF [$\lambda_{\text{max}}(\text{nm})(10^{-3}\epsilon(\text{dm}^3 \text{mol}^{-1} \text{cm}^{-1}))$]: 271 (7.10), 364 (7.08), 380 (10.60), 392 (10.90), 470 (0.44). $[\text{Pb}(\text{HaaiBz})(\text{I})_2]_n$ (**10a**): *Anal. Calc.* for $\text{C}_{16}\text{H}_{14}\text{I}_2\text{N}_4\text{Pb}$: C, 26.55; H, 1.94; N, 7.74. Found: C, 26.50; H, 1.90; N, 7.70%. FT-IR (KBr disc, cm^{-1}), $\nu(\text{N}=\text{N})$, 1435; $\nu(\text{C}=\text{N})$, 1599 cm^{-1} . UV–Vis spectral data in DMF [$\lambda_{\text{max}}(\text{nm})(10^{-3}\epsilon(\text{dm}^3 \text{mol}^{-1} \text{cm}^{-1}))$]: 293 (13.80), 300 (13.40), 362 (5.30), 385 (11.55), 465 (0.30). $[\text{Pb}(\text{MeaiBz})(\text{I})_2]_n$ (**10b**): *Anal. Calc.* for $\text{C}_{17}\text{H}_{16}\text{I}_2\text{N}_4\text{Pb}$: C, 27.67; H, 2.17; N, 7.60. Found: C, 27.60; H, 2.13; N, 7.67%. FT-IR (KBr disc, cm^{-1}), $\nu(\text{N}=\text{N})$, 1438; $\nu(\text{C}=\text{N})$, 1602 cm^{-1} . UV–Vis spectral data in DMF [$\lambda_{\text{max}}(\text{nm})(10^{-3}\epsilon(\text{dm}^3 \text{mol}^{-1} \text{cm}^{-1}))$]: 267 (10.70), 382 (13.40), 468 (0.40).

2.3.2. Synthesis of $[\text{Pb}(\text{MeaiMeBz})^+(\text{I}_3)^-]$ (**14b**)

To a methanolic solution (25 ml) of $[\text{MeaiMeBz}]^+\text{I}^-$ (1-methyl-3-benzyl-2-(*p*-tolylazo)imidazolium iodide) (**7b**) (0.2 g, 0.48 mmol), PbI_2 (0.22 g, 0.48 mmol) was added pinchwise and stirred and refluxed for 10 h. The solution was filtered hot through G4 crucible and slowly evaporated in air. Block shaped orange-red crystals were deposited on the wall of the beaker and collected by filtration. These crystals were ground and 2-methoxy-ethanol solution was prepared. Methanol (2 volume) was added into this solution. After a week bright orange-red colored block shaped crystals were separated and dried over CaCl_2 in a desiccator. The yield was 0.3 g (71%).

All other complexes were prepared by the same procedure. In all cases, crystalline products were obtained. The yield varied from 70% to 80% and microanalytical data of the complexes are as follows. $[\text{HaaiMe}_2][\text{PbI}_3]$ (**11a**):

Anal. Calc. for $C_{11}H_{13}I_3N_4Pb$: C, 16.73; H, 1.65; N, 7.10. Found: C, 16.66; H, 1.60; N, 7.05%. FT-IR (KBr disc, cm^{-1}), $\nu(N=N)$, 1432; $\nu(C=N)$, 1588 cm^{-1} . UV-Vis spectral data in DMF [$\lambda_{max}(nm)(10^{-3}\epsilon(dm^3 mol^{-1} cm^{-1}))$]: 268 (1.07), 287 (8.90), 364 (23.00), 386 (10.28), 420 (4.35). [MeaaiMe₂][PbI₃] (**11b**): *Anal. Calc.* for $C_{12}H_{15}I_3N_4Pb$: C, 17.93; H, 1.87; N, 6.97. Found: C, 18.00; H, 1.90; N, 7.05%. FT-IR (KBr disc, cm^{-1}), $\nu(N=N)$, 1445; $\nu(C=N)$, 1591 cm^{-1} . UV-Vis spectral data in DMF [$\lambda_{max}(nm)(10^{-3}\epsilon(dm^3 mol^{-1} cm^{-1}))$]: 270 (5.76), 353 (11.10), 381 (9.80), 397 (10.70), 400 (8.38). [HaaiEt₂][PbI₃] (**12a**): *Anal. Calc.* for $C_{13}H_{17}I_3N_4Pb$: C, 19.09; H, 2.08; N, 6.85. Found: C, 19.13; H, 2.12; N, 6.91%. FT-IR (KBr disc, cm^{-1}), $\nu(N=N)$, 1441; $\nu(C=N)$, 1596 cm^{-1} . UV-Vis spectral data in DMF [$\lambda_{max}(nm)(10^{-3}\epsilon(dm^3 mol^{-1} cm^{-1}))$]: 274 (4.62), 365 (10.00), 387 (8.75), 410 (5.80). [MeaaiEt₂][PbI₃] (**12b**): *Anal. Calc.* for $C_{14}H_{19}I_3N_4Pb$: C, 20.21; H, 2.29; N, 6.74. Found: C, 20.25; H, 2.24; N, 6.80%. FT-IR (KBr disc, cm^{-1}), $\nu(N=N)$, 1438; $\nu(C=N)$, 1594 cm^{-1} . UV-Vis spectral data in DMF [$\lambda_{max}(nm)(10^{-3}\epsilon(dm^3 mol^{-1} cm^{-1}))$]: 310 (3.55), 370 (8.20), 390 (8.00), 414 (7.55). [HaaiBz₂][PbI₃] (**13a**): *Anal. Calc.* for $C_{23}H_{21}I_3N_4Pb$: C, 29.32; H, 2.23; N, 5.95. Found: C, 29.40; H, 2.27; N, 6.05%. FT-IR (KBr disc, cm^{-1}), $\nu(N=N)$, 1440; $\nu(C=N)$, 1596 cm^{-1} . UV-Vis spectral data in DMF [$\lambda_{max}(nm)(10^{-3}\epsilon(dm^3 mol^{-1} cm^{-1}))$]: 270 (4.45), 350 (9.10), 388 (9.65), 397 (10.40), 428 (1.67). [MeaaiBz₂][PbI₃] (**13b**): *Anal. Calc.* for $C_{24}H_{21}I_3N_4Pb$: C, 30.15; H, 2.41; N, 5.86. Found: C, 30.10; H, 2.45; N, 5.80. FT-IR (KBr disc, cm^{-1}), $\nu(N=N)$, 1437; $\nu(C=N)$, 1594 cm^{-1} . UV-Vis spectral data in DMF [$\lambda_{max}(nm)(10^{-3}\epsilon(dm^3 mol^{-1} cm^{-1}))$]: 280 (5.45), 370 (10.50), 380 (9.90), 405 (5.85). [HaaiMe(Bz)][PbI₃] (**14a**): *Anal. Calc.* for $C_{17}H_{17}I_3N_4Pb$: C, 23.58; H, 1.96; N, 6.47. Found: C, 23.65; H, 2.00; N, 6.40%. FT-IR (KBr disc, cm^{-1}), $\nu(N=N)$, 1441; $\nu(C=N)$, 1597 cm^{-1} . UV-Vis spectral data in DMF [$\lambda_{max}(nm)(10^{-3}\epsilon(dm^3 mol^{-1} cm^{-1}))$]: 260 (4.75), 366 (8.80), 390 (10.80), 410 (7.67). [MeaaiMe(Bz)][PbI₃] (**14b**): *Anal. Calc.* for $C_{18}H_{19}I_3N_4Pb$: C, 24.57; H, 2.16; N, 6.37. Found: C, 24.55; H, 2.10; N, 6.40%. FT-IR (KBr disc, cm^{-1}), $\nu(N=N)$, 1445; $\nu(C=N)$, 1592 cm^{-1} . UV-Vis spectral data in DMF [$\lambda_{max}(nm)(10^{-3}\epsilon(dm^3 mol^{-1} cm^{-1}))$]: 310 (3.55), 365 (8.50), 378 (10.70), 440 (6.65).

2.4. X-ray crystal structure analyses

Crystals suitable for X-ray diffraction study of Pb(MeaaiMe)₂ (**8b**) and [1-Me-3-CH₂Ph-2-(*p*-tolylazo)imidazolium]⁺[PbI₃]⁻ (**14b**) were prepared by slow evaporation of *N,N*-dimethylformamide solution of compound along with few drops of methanol at ambient condition. Diffraction data were collected with the Bruker SMART 1K CCD area-detector diffractometer using fine focused sealed tube graphite-monochromatized Mo K α radiation ($\lambda = 0.71073 \text{ \AA}$). Unit cell parameters were determined from least-squares method with the data in the range of $-10 \leq$

Table 1

Summarised crystallographic data for [Pb(MeaaiMe)₂] (**8b**) and [MeaaiMe(CH₂Ph)⁺Pb(μ -I₃)⁻] (**14**)

	[Pb(MeaaiMe) ₂] (8b)	[MeaaiMe(CH ₂ Ph) ⁺ Pb(μ -I ₃) ⁻] (14)
Empirical formula	C ₁₁ H ₁₃ N ₄ I ₃ Pb	C ₁₈ H ₁₉ N ₄ I ₃ Pb
Formula weight	649.14	879.26
Temperature (K)	294	295
Crystal system	triclinic	triclinic
Space group	<i>P</i> $\bar{1}$	<i>P</i> $\bar{1}$
Crystal size (mm ³)	0.20 × 0.15 × 0.10	0.20 × 0.10 × 0.10
<i>Unit cell dimensions</i>		
<i>a</i> (Å)	8.3189(19)	8.109(11)
<i>b</i> (Å)	9.672(2)	11.322(16)
<i>c</i> (Å)	10.780(2)	13.618(19)
α (°)	71.522(4)	97.10(2)
β (°)	82.222(4)	94.45(3)
γ (°)	78.459(4)	103.92(2)
<i>V</i> (Å ³)	803.6(3)	1197(3)
<i>Z</i>	2	2
λ (Å)	0.71073	0.71073
μ (Mo K α) (mm ⁻¹)	12.562	10.929
<i>D</i> _{calc} (mg m ⁻³)	2.733	2.440
Refined parameters	163	238
Total reflections	8646	12763
Unique data [<i>I</i> > 2 σ (<i>I</i>)]	2779	3343
<i>R</i> ₁ ^a [<i>I</i> > 2 σ (<i>I</i>)]	0.0310	0.0320
<i>wR</i> ₂ ^b	0.0640	0.0854
Goodness-of-fit	0.96	0.846
Δ _{max} (e Å ⁻³)	1.18	0.554
Δ _{min} (e Å ⁻³)	-1.03	-1.078

^a $R = \sum |F_o - F_c| / \sum F_o$.

^b $wR = [\sum w(F_o^2 - F_c^2)^2 / \sum wF_o^4]^{1/2}$ are general but *w* are different, $w = 1/[\sigma^2(F_o^2) + (0.0695P)^2 + 0.0000P]$ for HaaiCH₂PhH⁺Cl⁻ · 2H₂O; $w = 1/[\sigma^2(F_o^2) + (0.0250P)^2 + (0.0000P)]$ for **8b** and $w = 1/[\sigma^2(F_o^2) + (0.0100P)^2 + (0.0000P)]$ for **14** where $P = (F_o^2 + 2F_c^2)/3$.

$h \leq 10$, $-12 \leq k \leq 12$, $-14 \leq l \leq 14$ and angle varies $4.0^\circ < 2\theta < 56.6^\circ$ for (**8b**); $-10 \leq h \leq 10$, $-15 \leq k \leq 14$, $-17 \leq l \leq 18$ and angle varies $3.04^\circ < 2\theta < 56.62^\circ$ for (**14b**). A summary of the crystallographic data and structure refinement parameters is given in Table 1. Data were corrected for Lorentz and polarization effects. Data reduction was carried out by using SAINT program. The structure was solved by direct methods using SHELXS-97 [36] and successive difference Fourier syntheses. All non-hydrogen atoms were refined anisotropically. Full matrix least-squares refinements on F_o^2 were carried out using SHELXL-97 [37] with anisotropic displacement parameters for all non-hydrogen atoms. Hydrogen atoms were constrained to ride on the respective carbon or nitrogen atoms with an isotropic displacement parameter equal to 1.2 times the equivalent isotropic displacement of their parent atom in all cases. All calculations were carried out using SHELXS-97 [36], PLATON 99 [38], and ORTEP-3 [39] programs.

3. Results and discussion

3.1. Synthesis and formulation

The ligands used are 1-alkyl-2-(arylazo)imidazole [RaaiR', where R = H (**a**), Me (**b**); R' = Me (**1**), Et (**2**),

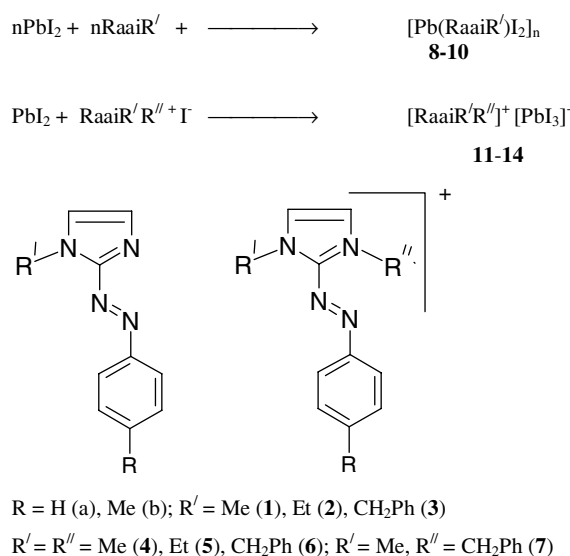
CH₂Ph (3)], they are unsymmetrical *N,N'*-bidentate chelator where *N* and *N'* refer to N(imidazole) and N(azo) donor centers, respectively. 1,3-Di-alkyl-2-(arylo)-imidazolium iodides (symmetrical: RaaiR'₂⁺I⁻, R' = Me, Me (4); Et, Et (5); CH₂Ph, CH₂Ph (6). Unsymmetrical: RaaiMe(CH₂Ph)⁺I⁻ (7)). The reaction between RaaiR' and PbI₂ in a 1:1 mole ratio in methanol and 2-methoxyethanol mixture has isolated polymeric [Pb(RaaiR')I₂]_n (R' = Me (8), Et (9), CH₂Ph (10)) compounds. The reaction between RaaiR'₂⁺I⁻ and PbI₂ under identical reaction conditions has synthesized tri-iodoplumbate, [RaaiR'₂⁺PbI₃⁻] (R' = Me (11), Et (12), CH₂Ph (13) and MeaaiMe(CH₂Ph)⁺PbI₃⁻ (14)].

3.2. Spectral studies

IR bands were assigned on comparing with free ligand data [40]. Moderately intense stretching at 1595–1600 and 1435–1445 cm⁻¹ is due to ν(C=N) and ν(N=N), respectively, for both types of complexes.

Very low solubility of [Pb(RaaiR')I₂]_n (8–10) in methanol and acetonitrile has ruled out to carry out the solution spectral studies. The complexes are soluble in DMF and the spectra are recorded in DMF solution. The ionic solids, [RaaiR'₂⁺][PbI₃⁻] (11–14), are soluble in acetonitrile and the solution electronic spectra were recorded in the wavelength range 250–900 nm. There are three bands and out of them two are high intense (ε ~ 10⁴ mol⁻¹ dm³ cm⁻¹) bands at 350–360 and 370–380 nm. On comparing with free ligand spectra [26–29,40], we may conclude that these bands are due to intramolecular charge transfer transitions. A weak band (ε ~ 10³ mol⁻¹ dm³ cm⁻¹) appears at 460–475 nm. This may be due to MLCT transition from Pb(II) → π*(azoimine).

The ¹H NMR spectra of [Pb(RaaiR')I₂] (8–10), [RaaiR'₂⁺][PbI₃⁻] (11–14) are recorded in CDCl₃. The atoms numbering patterns are shown in Scheme 1. Data (Table 2) reveal that the signals in the spectra of the complexes are shifted downfield relative to free ligand values. This supports the coordination of ligand to Pb(II). An important feature of the spectra is the shifting of imidazole protons 4-H and 5-H to lower δ-values, in general, relative to aryl protons (7-H–11-H). Imidazole protons suffer downfield shifting by 0.3–0.4 ppm compared to the free ligand position. This supports the strong preference of binding of imidazole-N to Pb(II). This property has been used to remove lead(II) from polluted water passing through azoimidazole



Scheme 1.

Table 2
¹H NMR spectral data in CDCl₃ at room temperature

Compound	δ, ppm (J, Hz)							
	4-H ^a	5-H ^a	7,11-H ^b	8-10-H	9-Me	1-(3-)-Me ^c	1-(3-)-CH ₂	(1-(3-)-CH ₂)CH ₃ ^f
[Pb(HaaiMe)(I ₂)] (8a)	7.55	7.22	7.88 (7.00)	7.60 ^c		4.01		
[Pb(HaaiEt)(I ₂)] (9a)	7.54	7.20	7.85	7.62 ^c			4.47 (9.0) ^d	1.55 (7.0)
[Pb(HaaiBz)(I ₂)] (10a) ^g	7.56	7.22	7.90 (7.0)	7.63 ^c			5.62 ^c	
[Pb(MeaaiMe)(I ₂)] (8b)	7.54	7.20	7.79 (7.00)	7.37 (7.00) ^b	2.48	3.97		
[Pb(MeaaiEt)(I ₂)] (9b)	7.52	7.20	7.75	7.35 (7.00) ^b	2.45		4.48 (9.0) ^d	1.55 (7.0)
[Pb(MeaaiBz)(I ₂)] (10b) ^g	7.53	7.20	7.80 (7.0)	7.40 ^c	2.45		5.60 ^c	
[HaaiMe ₂ ⁺][Pb(μ-I ₃) ⁻] (11a)	7.40	7.40	7.88 (7.0)	7.52 ^c		4.11		
[MeaaiMe ₂ ⁺][Pb(μ-I ₃) ⁻] (11b)	7.40	7.40	7.84 (7.0)	7.38 (7.0) ^b	2.44	4.14		
[HaaiEt ₂ ⁺][Pb(μ-I ₃) ⁻] (12a)	7.45	7.45	7.90 (7.0)	7.55 ^c			4.68 (10.0) ^d	1.52 (7.0)
[MeaaiEt ₂ ⁺][Pb(μ-I ₃) ⁻] (12b)	7.42	7.42	7.85 (7.0)	7.40 (7.00) ^b	2.42		4.70 (10.0)	1.55 (7.0)
[Haai(CH ₂ Ph) ₂ ⁺][Pb(μ-I ₃) ⁻] (13a) ^g	7.51	7.51	7.92 (7.0)	7.55 ^c			5.75 ^c	
[Meaai(CH ₂ Ph) ₂ ⁺][Pb(μ-I ₃) ⁻] (13b) ^g	7.50	7.50	7.90 (7.0)	7.42 (7.00) ^b	2.48		5.73 ^c	
[MeaaiMe(CH ₂ Ph) ⁺][Pb(μ-I ₃) ⁻] (14) ^g	7.49	7.49	7.96 (7.0)	7.36 (7.00) ^b	2.48		5.75 ^c	

^a Broad singlet.

^b Doublet.

^c Multiplet.

^d Quartet.

^e Singlet.

^f Triplet.

^g δ (Ph): 7.40–7.55 ppm, multiplet.

resin [41–43]. Aryl signals shift to the lower field side on Me-substitution to the aryl ring. This is due to electron donating effect of the Me-group. There is no noteworthy difference in the chemical shift data of $[\text{RaaiR}'\text{R}''\text{I}]^+\text{I}^-$ [44] and tri-iodo plumbate compounds (11–14).

3.3. Molecular structure

3.3.1. $[\text{Pb}(\text{MeaaiMe})\text{I}_2]_n$ (8b)

The structure of **8b** consists of 1D chain of alternating chelated lead(II) with MeaaiMe (1-methyl-2-(*p*-tolyl-

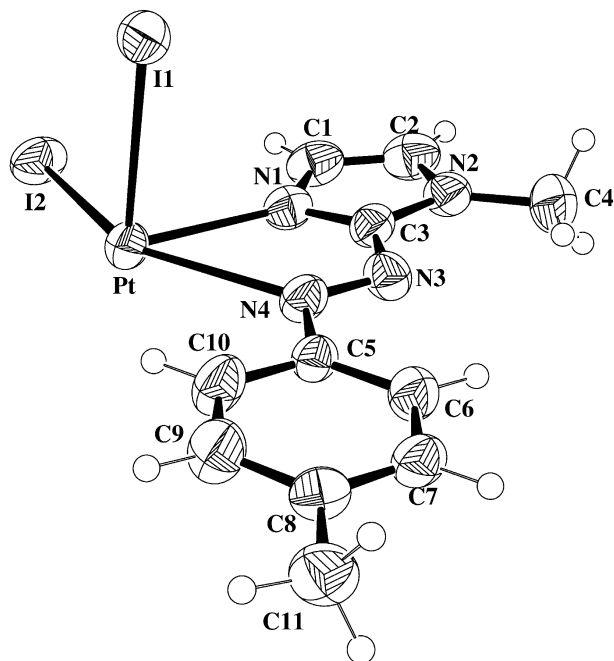


Fig. 1. ORTEP view of a fragment of $[\text{Pb}(\text{MeaaiMe})\text{I}_2]_n$.

lazo)imidazole) and iodine atoms. The monomeric unit of 1D chain is shown in Fig. 1 and the bond parameters are listed in Table 3. The structure shows non-planar asymmetrically bridged $-\text{Pb}(\mu\text{-I})_2\text{Pb}-$ units. Lead is located in a distorted octahedral environment with PbN_2I_4 coordination; two N donor centers, N(imidazole) and N(azo), are coming from chelated MeaaiMe ligand. The ligand lies on alternate side of each chain, which runs parallel to *c*-axis. The packing of molecular chains is illustrated in Fig. 2. The unsymmetrical nature of the ligand is reflected from the Pb–N bond distance data in the chelated structure: the Pb–N(imidazole), 2.477(5) Å is shorter than Pb–N(azo), 2.765(5) Å length. The distortion may be originated from small chelate angle $\angle\text{N}(1)\text{–Pb–N}(4)$, $61.92(16)^\circ$ and long

Table 3
Selected bond lengths and bond angles of $[\text{Pb}(\text{MeaaiMe})\text{I}_2]_n$ (8b)

Bond lengths (Å)		Bond angles ($^\circ$)	
Pb(1)–I(1)	3.0747 (5)	N(1)–Pb(1)–N(4)	61.92(16)
Pb(1)–I(2)	3.1378(8)	N(1)–Pb(1)–I(1)	87.53(12)
Pb(1)–I(1)*	3.4762(8)	N(4)–Pb(1)–I(1)	84.00(11)
Pb(1)–I(2)**	3.3336(7)	N(1)–Pb(1)–I(2)	86.73(12)
Pb(1)–N(1)	2.477(5)	N(4)–Pb(1)–I(2)	148.63(11)
Pb(1)–N(4)	2.765(5)	I(1)–Pb(1)–I(2)	96.458(17)
N(3)–N(4)	1.258(7)	N(1)–Pb(1)–I(2)*	84.46(12)
N(3)–C(3)	1.399(8)	N(4)–Pb(1)–I(2)*	79.72(11)
N(4)–C(5)	1.413(8)	I(1)–Pb(1)–I(2)*	163.716(15)
		I(2)–Pb(1)–I(2)*	97.213(18)
		N(1)–Pb(1)–I(1)**	169.44(12)
		N(4)–Pb(1)–I(1)**	107.64(11)
		I(1)–Pb(1)–I(1)**	89.78(2)
		I(2)–Pb(1)–I(1)**	95.52(2)
		Pb(1)–I(1)**–Pb(2)	90.22(2)
		Pb(1)–I(2)*–Pb(2)	82.787(18)

Symmetry: *1 – X, 1 – Y, 1 – Z; **–X, 1 – Y, 1 – Z.

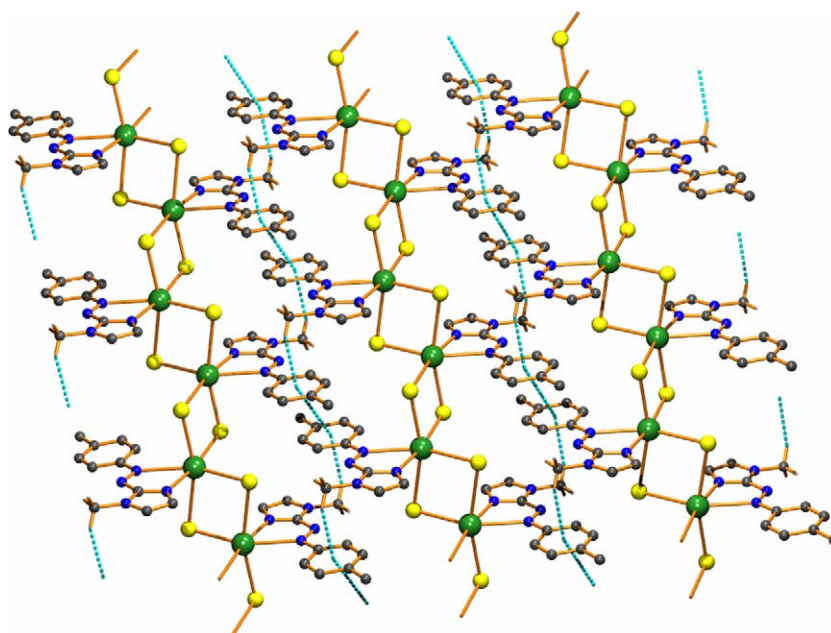


Fig. 2. π -Sheet of $[\text{Pb}(\text{MeaaiMe})\text{I}_2]_n$, showing both C–H $\cdots\pi$ and $\pi\cdots\pi$ interactions amongst inter-chain components.

Pb–N(azo) distance. The elongation of the Pb–N(azo) distance may have several reasons. First, the N(azo) belongs to exocyclic N=N along with a pendant aryl group; thus the van der Waals repulsion will be greater than N(imidazole). Second, the N(azo) has larger s-character compared to N(imidazole) and thus it is more space demanding. Besides, the presence of the lone pair results in a non-spherical charge distribution around Pb(II) in solids to lower the symmetry of the coordination of the negative ions around them [45,46]. Although Pb–N(azo) (2.765(5) Å) is longer than Pb–N(imidazole) (2.477(5) Å) but it is shorter than the sum of van der Waals radii of Pb (2.02 Å) and N(azo) (1.55 Å). This implies covalent interaction between Pb(II) and N(azo).

In {PbI₄} unit Is are bridged in pairs with adjacent Pb(II) centers at either side of the central unit (Fig. 2). Each chelating ligand, MeaaiMe, about Pb in the bridged dimer is oriented in such a fashion that two N(azo) centers are either coming closer or moving away from each other. The Pb–I distances (3.0747–3.4762 Å) lie in the range of the reported data [47,48]. The azo N=N bond length in chelated MeaaiMe is 1.258(8) Å. This is slightly elongated than that of free ligand value (1.251(7) Å) [49]. The short Pb–N(imidazole) bond length compared to Pb–N(azo) distance is in support of preferential stronger interaction of Pb(II) with N(imidazole). Lead(II) is one of the heavy metals exhibiting very high biochemical toxicity and carcinogenicity due to its binding to –SH group to a class of thiol

proteins [50,51]. It inhibits heme synthesis and causes anaemia. Imidazole is present in most of the biomolecular nucleic acids, proteins, DNA, and the preferential binding of Pb(II) to imidazole–N may be the reason for very high toxic efficiency of lead(II). The pendant phenyl ring of each chelated MeaaiMe in the 1D chain of alternate molecular fragment, Pb(MeaaiMe), penetrates into the groove of neighbouring 1D chain. This ascertains a $\pi \cdots \pi$ interaction

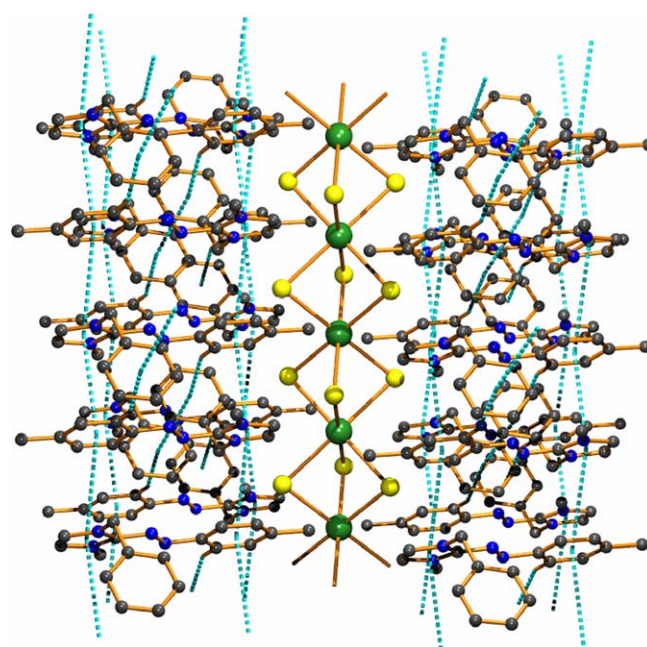


Fig. 4. Anion polymer of $[PbI_6]^{4-}$ penetrated into π -pillars constituted by $[MeaaiMe(CH_2Ph)]_n^+$ through hydrogen bonding interaction.

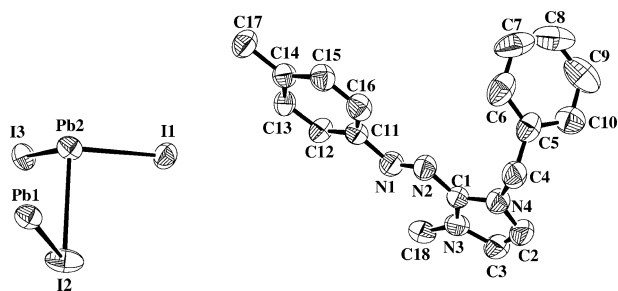


Fig. 3. ORTEP view of ionic solid $[MeaaiMe(CH_2Ph)]^+[PbI_3]^-$.

Table 4

Selected bond lengths and bond angles of $[MeaaiMe(CH_2Ph)]^+[PbI_3]^-$ (**14b**)

Bond lengths (Å)		Bond angles (°)	
Pb(1)–I(2)	3.230(3)	I(2)–Pb(1)–I(2)#2	180.00
Pb(1)–I(1)#1	3.244(3)	I(2)–Pb(1)#2–I(1)#1	85.8(1)
Pb(1)–I(3)#1	3.251(3)	I(2)–Pb(1)–I(3)#1	95.6(1)
Pb(2)–I(2)	3.232(3)	I(1)–Pb(1)#1–I(3)#1	83.86(6)
Pb(2)–I(1)	3.235(3)	I(2)–Pb(1)–I(3)#2	84.4(1)
Pb(2)–I(3)#2	3.219(3)	I(2)–Pb(1)–I(1)#1	94.3(1)
N(1)–N(2)	1.26(1)	I(1)–Pb(1)#2–I(3)#1	96.14(6)
N(2)–C(1)	1.41(1)	I(3)–Pb(2)–I(1)	84.52(8)
N(1)–C(11)	1.45(1)	I(3)–Pb(2)–I(1)#2	95.48(8)
		Pb(2)–I(1)–Pb(1)#1	77.5(1)
		I(3)–Pb(2)#2–I(1)#2	84.52(8)
		Pb(1)–I(2)–Pb(2)	77.7(1)

Symmetry operators: #1 x, y, z ; #2 $-x, -y, -z$.

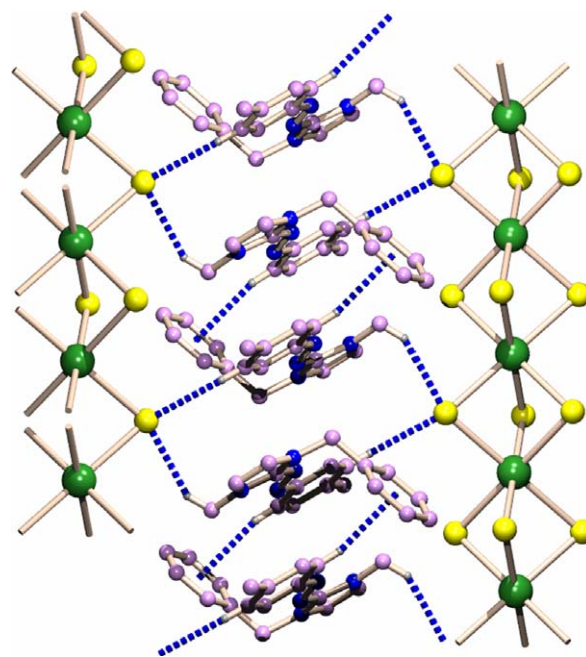


Fig. 5. $[MeaaiMe(CH_2Ph)]^+$ s are flanked between $[PbI_6]_n$ pillars by bifurcated C–H \cdots I \cdots H–C interactions. Organic units also show intermolecular C–H \cdots π interaction to stabilize the layer.

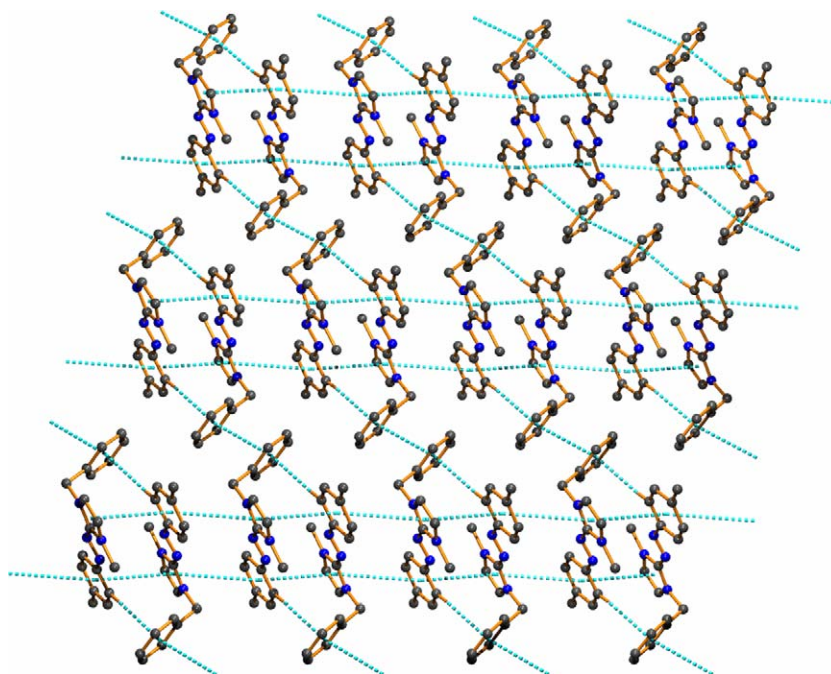


Fig. 6. View of π -sheet through C–H $\cdots\pi$, face-to-face $\pi\cdots\pi$ interaction in $[\text{MeaaiMe}(\text{CH}_2\text{Ph})]_n^+$ (for clarity $(\text{PbI}_3)^-$ is omitted).

with pendant *p*-tolyl rings and imidazole groups. The interaction is weak (Centroid (Cg) \cdots Centroid (Cg) distance of *p*-tolyl \cdots *p*-tolyl, 4.012(4) Å; imidazole \cdots *p*-tolyl, 4.32(4) Å), but the disposition of rings warrants to consider that the arrangement is a 2D network (Fig. 2). The existence of inter-chain C–H $\cdots\pi$ interaction (considering H or C \cdots Centroid (Cg) of *p*-Tol ring (Imz-N-CH₃) C(4)–H(4) \cdots *p*-Tol(2) (symmetry: 1 – X, 1 – Y, –Z): H–*p*-Tol, 2.78 Å; C \cdots *p*-Tol, 3.556(9) Å; \angle C–H \cdots *p*-Tol, 138°) constitutes formal π -sheet as it is shown in Fig. 2.

3.3.2. $[\text{MeaaiMe}(\text{CH}_2\text{Ph})]_n^+ [\text{PbI}_3]^-$ (14)

The molecular unit is shown in Fig. 3 and bond parameters are listed in Table 4. The structure is constituted from iodo-bridged $[\text{PbI}_6]_n$ anion polymer and $[\text{MeaaiMe}(\text{CH}_2\text{Ph})]_n^+$ (Fig. 4). The polymer is constituted by six Pb–I–Pb bridging and generates distorted octahedral PbI_6 coordination arrangement. There are three different Pb–I bond distances in between two Pb centers (Pb1 and Pb2). The Pb–I distances lie in the reported range, 3.2–3.4 Å. The anion chains are hydrogen bonded to 1-methyl-3-benzyl-2-(*p*-tolylazo)imidazolium ($\text{MeaaiCH}_2\text{PhMe}^+$) ions forming neutral sheets perpendicular to *b*. The organic cations are placed in between the parallel pillars of $[\text{PbI}_6]_n$ and are held by hydrogen bonds with bridged-I (C(15)–H(15) \cdots I(2e): C–H, 0.930; H \cdots I, 3.030(1); C \cdots I, 3.884(11) Å and \angle C–H \cdots I, 152.77° (symmetry: *x*, 1 + *y*, *z*); C(18)–H(18B) \cdots I(2f): C–H, 0.960; H \cdots I, 2.990(1); C \cdots I, 3.830(12) Å; \angle C–H \cdots I, 147.20° (symmetry: –*x*, –*y*, –*z*)) (Fig. 5). In C(18) \cdots H(18A) \cdots N(1): C–H, 0.960; H \cdots N, 2.220(1); C \cdots N, 2.906(12) Å and \angle C–H \cdots N, 128.00° (symmetry: *x*, 1 + *y*, *z*). The hydrogen bondings in C–H \cdots I pattern are scarce [52,53]. Both face-to-face

(Fig. 6) and edge-to-face (Fig. 7) $\pi\cdots\pi$ stacking interactions are observed between aromatic rings belonging to adjacent chains in the network. Azoimidazolium unit contains three different aromatic rings: *p*-tolyl (*p*-Tol), phenyl (Ph) and imidazole (Imz). The $\pi\cdots\pi$ interactions are appropriate to Centroid (Cg) \cdots Centroid (Cg) distance of Imz(2) \cdots *p*-Tol(1) (3.602(8) Å and dihedral, 4.53°) and Imz(1) \cdots *p*-Tol(2) (3.872(8) Å and dihedral, 4.53°) (1 and 2 in braces refer to two different molecules at adjacent). These two interactions lead to form 1-D π -chain. The π -chains exhibit C–H $\cdots\pi$ interactions (H or C \cdots Centroid (Cg) of Ph): C(12)–H(12) \cdots Ph(2): H(12) \cdots Ph(2), 2.83 Å; C(12) \cdots Ph(2), 3.687(11) Å; \angle C–H \cdots Ph, 154° where Ph(2) is coming from N-CH₂Ph in the molecule of adjacent chain (symmetry: –1 – X, 1 – Y, –Z). Inter-chain face-to-face $\pi\cdots\pi$ interaction between (N-CH₂)Ph \cdots Ph(CH₂-N) (Centroid \cdots Centroid distance is 3.711(9) Å; parallel) enables

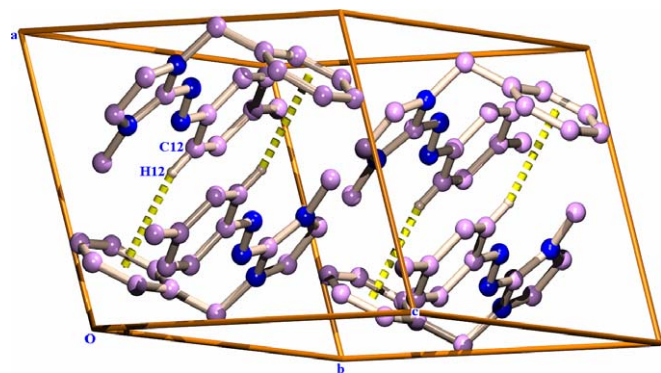


Fig. 7. Edge-to-face C–H $\cdots\pi$ (Cg) interaction. The least distance (C12 to the center of Ring1) is 3.627 Å.

to form a π -sheet. Parallel arrays of the planes of the aromatic moieties (Fig. 6) indicate that these interactions are of the face-to-face “ π -stacking” type [54,55]. There is also edge-to-face π -stacking interaction between *p*-Tol(1)··Ph(2) and the distance is 3.627 Å (Fig. 7) [56,57].

4. Conclusion

The work describes structural differences of di-iodo-Pb(II)-arylaizimidazoles and arylazimidazolium tri-iodoplumbate. The former gives iodo bridged 1-D neutral chain where arylazimidazole acts as an end capper. In the latter compound, anion polymer is generated by iodo bridging in tri-iodoplumbate where arylazimidazolium cation is intercalated by hydrogen bonding and $\pi \cdots \pi$ forces. The NMR, UV–Vis and IR spectral data also characterize the compounds.

5. Supplementary material

Crystallographic data for the structural analysis have been deposited with the Cambridge Crystallographic Data Centre; the CCDC Nos. for **8b** and **14** are 298934 and 298933, respectively. Copies of the information may be obtained free of charge from the Director, CCDC, 12 Union Road, Cambridge, CB2 1EZ, UK (fax: +44 1223 336033; e-mail: deposit@ccdc.com.ac.uk or www.ccdc.cam.ac.uk).

Acknowledgements

Financial supports (CS) from the DST and CSIR, New Delhi, are gratefully acknowledged. K.K.S. acknowledges CSIR for a fellowship.

References

- [1] D. Braga, F. Grepioni, A.G. Orpen, *Crystal Engineering: From Molecules and Crystals to Materials*. A NATO Advanced Study Institute and Euroconference, Erice, 1999, p. 58.
- [2] G.R. Desiraju, in: J.M. Lehn (Ed.), *The Crystals as a Supramolecular Entity*, vol. 2, Wiley, Chichester, UK, 1996.
- [3] B.F. Abrahams, S.R. Batten, H. Hamit, B.F. Hoskins, R. Robson, *Angew. Chem., Int. Ed. Engl.* 35 (1996) 1690.
- [4] C. Janiak, *Dalton Trans.* (2003) 2781.
- [5] S.L. James, *Chem. Soc. Rev.* 32 (2003) 276.
- [6] S. Kitagawa, R. Kitaura, S.-I. Noro, *Angew. Chem., Int. Ed.* 116 (2004) 2388.
- [7] S.-L. Zheng, X.-M. Chen, *Aust. J. Chem.* 57 (2004) 703.
- [8] D. Maspocho, D. Ruiz-Molina, J. Veciana, *J. Mater. Chem.* 14 (2004) 2713.
- [9] S.R. Batten, K.S. Murray, *Coord. Chem. Rev.* 246 (2003) 103.
- [10] F.A. Cotton, G. Wilkinson, C.A. Murillo, M. Bochmann, *Advanced Inorganic Chemistry*, sixth ed., John Wiley, New York, 1999.
- [11] H. Strasdeit, W. Saak, S. Pohl, W.L. Driessen, J. Reedijk, *Inorg. Chem.* 27 (1988) 1557.
- [12] Y.Y. Niu, H.G. Zheng, H.K. Fun, I.A. Razak, S. Chantrapromma, X.Q. Xin, *Synth. React. Inorg. Met. Org. Chem.* 33 (2003) 1.
- [13] C. Janiak, L. Uehlin, H.-P. Wu, P. Klufers, H. Piotrowski, T.G. Scharmann, *J. Chem. Soc., Dalton Trans.* (1999) 3121, and references in there.
- [14] P. Ren, J. Qin, T. Liu, S. Zhang, *Inorg. Chem. Commun.* 7 (2004) 134.
- [15] Y.Y. Niu, Y.-L. Song, J. Wu, H. Hou, Y. Zhu, X. Wang, *Inorg. Chem. Commun.* 7 (2004) 471.
- [16] M.R. Tubbs, A.J. Forty, *J. Appl. Phys.* 15 (1964) 1553.
- [17] J. Parr, *Polyhedron* 16 (1997) 551.
- [18] L. Shimoni-livny, J.P. Glusser, C.W. Brock, *Inorg. Chem.* 37 (1998) 1853.
- [19] C. Janiak, S. Temizdemir, T.G. Scharmann, A. Schmalstieg, J. Demtschuk, *Z. Anorg. Allg. Chem.* 626 (2000) 2053.
- [20] A. Morsali, X.-M. Chem, *J. Coord. Chem.* 57 (2004) 1253.
- [21] A. Morsali, A.R. Mahjoub, M.J. Soltanian, P.E. Pour, *Z. Naturforsch.* 60b (2005) 300.
- [22] U.S. Ray, B.K. Ghosh, M. Monfort, J. Ribas, G. Mostafa, T.-H. Lu, C. Sinha, *Eur. J. Inorg. Chem.* (2004) 250.
- [23] U.S. Ray, B.G. Chand, G. Mostafa, J. Cheng, T.-H. Lu, C. Sinha, *Polyhedron* 22 (2003) 2587.
- [24] D. Banerjee, U.S. Ray, J.-C. Liou, C.-N. Lin, T.-H. Lu, C. Sinha, *Inorg. Chim. Acta* 358 (2005) 1019.
- [25] U.S. Ray, D. Banerjee, B.G. Chand, J. Cheng, T.-H. Lu, C. Sinha, *J. Coord. Chem.* 58 (2005) 1105.
- [26] B.G. Chand, U.S. Ray, J. Cheng, T.-H. Lu, C. Sinha, *Polyhedron* 22 (2003) 1213.
- [27] B.G. Chand, U.S. Ray, G. Mostafa, T.-H. Lu, C. Sinha, *Polyhedron* 23 (2004) 1669.
- [28] B.G. Chand, U.S. Ray, G. Mostafa, T.-H. Lu, C. Sinha, *J. Coord. Chem.* 57 (2004) 627.
- [29] B.G. Chand, U.S. Ray, J. Cheng, T.-H. Lu, C. Sinha, *Inorg. Chim. Acta* 358 (2005) 1927.
- [30] C. Janiak, *J. Chem. Soc., Dalton Trans.* (2000) 3885.
- [31] M. Nishio, *Cryst. Eng. Commun.* 6 (2004) 130.
- [32] M. Nishio, M. Hirota, Y. Umezawa, *The CH/ π Interaction (Evidence, Nature and Consequences)*, Wiley-VCH, New York, 1998.
- [33] C. Janiak, S. Temizdemir, S. Dechert, W. Deck, F. Girgsdies, J. Heinze, M.J. Kolm, T.G. Scharmann, O.M. Zippel, *Eur. J. Inorg. Chem.* (2000) 1229.
- [34] U.S. Ray, G. Mostafa, T.H. Lu, C. Sinha, *Cryst. Eng.* 5 (2002) 95.
- [35] U.S. Ray, B.G. Chand, A.K. Dasmahapatra, G. Mostafa, T.-H. Lu, C. Sinha, *Inorg. Chem. Commun.* 6 (2003) 634.
- [36] G.M. Sheldrick, *SHELXS-97 Program for the Solution of Crystal Structure*, University of Gottingen, Germany, 1997.
- [37] G.M. Sheldrick, *SHELXL-97 Program for the Refinement of Crystal Structure*, University of Gottingen, Germany, 1997.
- [38] A.L. Spek, *PLATON, Molecular Geometry Program*, University of Utrecht, The Netherlands, 1999.
- [39] L.J. Farrugia, *J. Appl. Crystallogr.* 30 (1997) 65.
- [40] T.K. Misra, Ph.D. Thesis, Burdwan University, Burdwan, India, 1997.
- [41] D. Das, A.K. Das, C. Sinha, *Talanta* 48 (1999) 1013.
- [42] D. Das, A.K. Das, C. Sinha, *Anal. Lett.* 32 (1999) 567.
- [43] P. Chattopadhyay, C. Sinha, D.K. Pal, *Fresenius J. Anal. Chem.* 357 (1997) 368.
- [44] T. Mathur, Ph.D. Thesis, Burdwan University, Burdwan, India, 2005.
- [45] D.L. Reger, M.F. Huff, A.L. Rheingold, B.S. Haggerty, *J. Am. Chem. Soc.* 114 (1992) 579.
- [46] A.A. Soudi, F. Marandi, A. Morsali, L.-G. Zhu, *Inorg. Chem. Commun.* 8 (2005) 773.
- [47] H.-G. Zhu, Y. Xu, Z. Yu, Q.-J. Wu, H.-K. Fun, X.-Z. You, *Polyhedron* 18 (1999) 3491.
- [48] S. Wang, D.B. Mitzi, C.A. Field, A. Guloy, *J. Am. Chem. Soc.* 117 (1995) 5297.
- [49] P. Bhunia, B. Baruri, U.S. Ray, C. Sinha, S. Das, J. Cheng, T.-H. Lu, *Trans. Met. Chem.* 31 (2006) 310.
- [50] S.E. Manhan, *Environmental Chemistry*, fourth ed., Lewis Publishers, Boston, 1990.
- [51] J.E. Fergusson, *The Heavy Elements: Chemistry, Environmental Impact and Health Effects*, Pergamon Press, Oxford, 1990.

- [52] H. Karutscheid, F. Vielsack, K.N. Frieder, *Z. Anorg. Alleg. Chem.* 624 (1998) 807.
- [53] S.J. Garden, C. Glidewell, J.N. Low, J.M.S. Skakle, J.L. Wardell, *Acta Crystallogr. Sect. C, Cryst. Struct. Commun.* C61 (2005) 145.
- [54] I.G. Dance, M.L. Scudder, *J. Chem. Soc., Dalton Trans.* (1996) 3755.
- [55] Z.-H. Liu, C.-Y. Duan, J.-H. Li, Y.-J. Liu, Y.-H. Mei, X.-Z. You, *New J. Chem.* 24 (2000) 1057.
- [56] C.A. Hunter, J.K.M. Sanders, *J. Am. Chem. Soc.* 112 (1990) 5525.
- [57] C. Janiak, *J. Chem. Soc., Dalton Trans.* (2000) 3885.